Demodulation Algorithm Based on Higher Order Synchrosqueezing

Duong-Hung Pham, Sylvain Meignen

Demodulation Algorithm Based on Higher Order Synchrosqueezing

Duong-Hung Pham
Laboratoire ICube - UMR 7357 CRNS
300 bd Sébastien Brant - CS 10413 - F-67412 Illkirch Cedex
dhpham@unistra.fr

Sylvain Meignen
Laboratoire Jean Kuntzmann - UMR 5224 CNRS
700 Avenue Centrale, 38401 Saint-Martin-d'Hères, France
sylvain.meignen@univ-grenoble-alpes.fr

***Abstract*—This paper addresses the problem of detecting and retrieving amplitude- and frequency-modulated (AM-FM) components or modes of a multicomponent signal from its time-frequency representation (TFR) corresponding to its short-time Fourier transform. For that purpose, we introduce a novel technique that combines a high order synchrosqueezing transform (FSSTN) with a demodulation procedure. Numerical results on a multicomponent signal, both in noise-free and noisy cases, show the benefits for mode reconstruction of the proposed approach over similar techniques that do not make use of demodulation.**

***Index Terms*—time-frequency analysis, AM-FM mode, multicomponent signals, synchrosqueezing techniques, demodulation.**

I. Introduction

Multicomponent signals (MCSs), defined as sums of amplitude- and frequency-modulated (AM-FM) waves, have received great interest from the signal processing community over the last decades because of their ability to accurately represent *non-stationary* signals arising from a wide range of applications e.g., audio recordings, structural stability [1], [2], or physiological signals [3]. Time-frequency (TF) representations (TFRs) play a central role for characterizing such signals, among which the *continuous wavelet transform* (CWT) and the *short-time Fourier transform* (STFT) are the most popular [4]. However, the effectiveness of these transforms is constrained by the choice of window or wavelet. Indeed, the *Heisenberg uncertainty principle* limits both the adaptivity and the readability of these TFRs. To improve the readability, a *reassignment method* (RM) was proposed by Kodera *et al.* [5] in the 1970s and then further developed in [6]. Unfortunately, the reassigned representation given by RM was not invertible: when applied to an MCS, it did not allow for easy retrieval of signal components. Alternatively, a technique using the same principle as RM but keeping the invertibility property, and known as the *synchrosqueezing transform* (SST), was developed in the wavelet framework [7], and then theoretically studied in [8]. In essence, the retrieval procedure consists of estimating, on the TFR associated with the modulus of CWT, so-called *ridges* which are estimators of the instantaneous frequencies (IFs) of the modes, reassigning the transform in the vicinity of the detected ridges, and finally inverting the reassigned transform. Such an approach was then adapted to the TFR given by STFT in [9], and is now known as the *STFT-based synchrosqueezing transform* (FSST). However, all these transforms suffer from a serious limitation which is that they cannot deal with modes containing strong frequency modulations, commonly encountered in real-world situations e.g., radar [10], speech processing [11], or gravitational waves [12], [13]. To better handle this case, an extension of FSST known as the *second-order* FSST (FSST2) was proposed in [14] and its theoretical foundations settled in [15]. Moreover, this new transform was recently used in conjunction with a *demodulation operator* leading to better mode reconstruction results [16]. FSST2 was also further extended to better deal with modes with very fast oscillating phase and denoted by FSSTN with N = 3, 4,... [17]. To investigate how the combination of FSSTN with a demodulation operator can be beneficial to mode reconstruction is the main goal of the present paper.

To this end, after having recalled some useful background associated with SST in Section II, we revisit the idea of the demodulation algorithm based on FSST (or FSST2) for mode reconstruction and then detail its variant based on FSSTN context in Section III. Finally, we provide, in Section IV, numerical simulations, involving both noise-free and noisy MCSs, to demonstrate the improvement brought by the proposed approach over some state-of-the-art methods.

II. Background to Synchrosqueezing Transforms

Prior to starting, we recall useful notation, definitions and basic elements related to synchrosqueezing transforms.

A. Basic Notation and Definitions

Consider a signal $f \in L^1(\mathbb{R})$, its *Fourier transform* corresponds to:

$$\widehat{f}(\xi) = \mathcal{F}\{f\}(\xi) = \int_{\mathbb{R}} f(t) e^{-i2\pi\xi t} dt, \tag{1}$$

and its *short-time Fourier transform* (STFT) is defined using any sliding window $g \in L^\infty(\mathbb{R})$ by:

$$\begin{aligned} V_f^g(t,\xi) &= \int_{\mathbb{R}} f(\tau) g(\tau - t) e^{-2i\pi\xi(\tau - t)} d\tau \\ &= \int_{\mathbb{R}} f(t+\tau) g(\tau) e^{-2i\pi\xi\tau} d\tau. \end{aligned} \tag{2}$$

If $f, \hat{f}, g$ and $\hat{g}$ are all in $L^1(\mathbb{R})$, f can be reconstructed from its STFT as soon as g is non-zero at 0:

$$f(t) = \frac{1}{\overline{g(0)}} \int_{\mathbb{R}} V_f^g(t,\xi) d\xi, \tag{3}$$

where $\overline{Z}$ denotes the complex conjugate of Z.

In this paper, we will intensively study multicomponent signals (MCSs) defined as a superimposition of AM-FM components or modes:

$$f(t) = \sum_{k=1}^{K} f_k(t) \quad \textit{with} \quad f_k(t) = A_k(t) e^{i2\pi\phi_k(t)}, \tag{4}$$

for some finite $K \in \mathbb{N}$, $A_k(t)$ and $\phi_k'(t)$ being respectively the instantaneous amplitude (IA) and frequency (IF) f_k satisfying: $A_k(t) > 0, \phi_k'(t) > 0$ and $\phi_{k+1}'(t) > \phi_k'(t)$ for all t. Such a signal admits an ideal TF (ITF) representation defined as:

$$\mathrm{TI}_f(t,\omega) = \sum_{k=1}^{K} A_k(t) \delta\left(\omega - \phi_k'(t)\right), \tag{5}$$

where δ denotes the Dirac distribution. In practice, the IF of the modes cannot be recovered by estimating the IF of f as is done in the theory of analytical signals, and to locate the modes in the TF plane is essential before computing their IFs: this is one of the goals of SST whose construction is recalled hereafter.

B. STFT-based synchrosqueezing transform

The STFT based synchrosqueezing (denoted by FSST in the sequel) starts with defining the *local instantaneous frequency* $\hat{\omega}_f$, wherever $V_f^g(t,\xi) \neq 0$, by [6]:

$$\widehat{\omega}_f(t,\xi) = \frac{\partial \arg V_f^g(t,\xi)}{\partial t} = \Re\left\{ \frac{1}{2i\pi} \frac{\partial_t V_f^g(t,\xi)}{V_f^g(t,\xi)} \right\}. \tag{6}$$

The FSST of f with threshold γ is obtained by moving any coefficient $V_f^g(t,\xi)$ with magnitude larger than γ to location $(t, \hat{\omega}_f(t,\xi))$. One then define the *synchrosqueezing transform* as:

$$T_f^\gamma(t,\omega) = \int_{|V_f^g(t,\xi)|>\gamma} V_f^g(t,\xi) \delta(\omega - \widehat{\omega}_f(t,\xi)) d\xi. \tag{7}$$

Any mode f_k can then be reconstructed by summing FSST coefficients around the k^{th} ridge, which amounts to modifying the synthesis formula (3) to select only the coefficients related to the k^{th} mode, namely:

$$f_k(t) \approx \frac{1}{\overline{g(0)}} \int_{|\omega - \varphi_k(t)|<d} T_f^\gamma(t,\omega) d\omega, \tag{8}$$

where φ_k is an estimation of ϕ_k', and parameter d is used to compensate for errors in IF estimation; it should be kept small enough to avoid mode-mixing, and its influence will be discussed later.

C. Second order synchrosqueezing transforms

The applicability of FSST is however restricted to a class of MCSs composed of slightly perturbed purely harmonic modes. To overcome this limitation, an extension of FSST, called *second-order STFT-based synchrosqueezing transform* (FSST2) [15], [18], was introduced based on a more accurate IF estimate than $\hat{\omega}_f$. More precisely, one first defines a *second-order local modulation operator* used to compute the new IF estimate. To do so, one introduces *complex reassignment operators* $\tilde{\omega}_f(t,\xi) = \frac{\partial_t V_f^g(t,\xi)}{2i\pi V_f^g(t,\xi)}$ and $\tilde{t}_f(t,\xi) = t - \frac{\partial_\xi V_f^g(t,\xi)}{2i\pi V_f^g(t,\xi)}$, and then defines a complex frequency modulation operator as [18]:

$$\tilde{q}_f(t,\xi) = \frac{\partial_t \tilde{\omega}_f(t,\xi)}{\partial_t \tilde{t}_f(t,\xi)} = \frac{\partial_t \left(\frac{\partial_t V_f^g(t,\xi)}{V_f^g(t,\xi)} \right)}{2i\pi - \partial_t \left(\frac{\partial_\xi V_f^g(t,\xi)}{V_f^g(t,\xi)} \right)}. \tag{9}$$

The second-order local modulation operator then corresponds to $\Re\{\tilde{q}_f(t,\xi)\}$, and the second order complex IF estimate of f is defined by:

$$\tilde{\omega}_f^{[2]}(t,\xi) = \begin{cases} \tilde{\omega}_f(t,\xi) + \tilde{q}_f(t,\xi)(t - \tilde{t}_f(t,\xi)) \text{ if } \partial_t \tilde{t}_f(t,\xi) \neq 0 \\ \tilde{\omega}_f(t,\xi) \text{ otherwise,} \end{cases} \tag{10}$$

and one then puts $\hat{\omega}_f^{[2]}(t,\xi) = \Re\left\{ \tilde{\omega}_f^{[2]}(t,\xi) \right\}$. It was proven in [15] that $\hat{\omega}_f^{[2]}(t,\xi) = \phi'(t)$, when f is a Gaussian modulated linear chirp. It is also worth mentioning here that $\tilde{q}_f(t,\xi)$ can be computed by means of five different STFTs. Finally, FSST2 is defined by replacing $\hat{\omega}_f(t,\xi)$ by $\hat{\omega}_f^{[2]}(t,\xi)$ in (7), to obtain the so-called $T_{2,f}^\gamma$, and mode reconstruction is then performed by replacing T_f^γ by $T_{2,f}^\gamma$ in (8).

D. Higher order synchrosqueezing transforms

Despite FSST2 definitely sharpens the TFR it is based on, it is proven to provide a truly sharp TFR only for perturbations of linear chirps with Gaussian modulated amplitudes. To handle signals containing more general types of AM-FM modes having non-negligible $\phi_k^{(k)}(t)$ for $k \geq 3$, especially those with fast oscillating phase, one defines new SST operators based on third- or higher-order approximations of both amplitude and phase [17]. To introduce the technique, we restrict ourselves to the STFT context but the technique presented hereafter could easily be extended to the CWT setting. Let $f(\tau) = A(\tau) e^{i2\pi\phi(\tau)}$ with $A(\tau)$ (*resp.* $\phi(\tau)$) being equal to its L^{th}-order (*resp.* N^{th}-order) Taylor expansion for τ close to t, namely:

$$\log(A(\tau)) = \sum_{k=0}^{L} \frac{[\log(A)]^{(k)}(t)}{k!} (\tau - t)^k$$
$$\text{and } \phi(\tau) = \sum_{k=0}^{N} \frac{\phi^{(k)}(t)}{k!} (\tau - t)^k, \tag{11}$$

where $Z^{(k)}(t)$ denotes the k^{th} derivative of Z evaluated at t. Such a mode, with $L \leq N$, can be written as:

$$f(\tau) = \exp\left(\sum_{k=0}^{N} \frac{1}{k!}\left([\log(A)]^{(k)}(t) + i2\pi\phi^{(k)}(t)\right)(\tau - t)^k\right), \tag{12}$$

since $[\log(A)]^{(k)}(t) = 0$ if $L+1 \leq k \leq N$. Its corresponding STFT reads:

$$V_f^g(t,\xi) = \int_{\mathbb{R}} \exp\left(\sum_{k=0}^{N} \frac{1}{k!}\left([\log(A)]^{(k)}(t) + i2\pi\phi^{(k)}(t)\right)\tau^k\right) g(\tau)e^{-i2\pi\xi\tau}d\tau.$$

Taking the partial derivative of $V_f^g(t,\xi)$ with respect to t and then dividing by $i2\pi V_f^g(t,\xi)$, the local complex reassignment operator $\tilde{\omega}_f(t,\xi)$ defined in Section II-C can be written, when $V_f^g(t,\xi) \neq 0$, as:

$$\tilde{\omega}_f(t,\xi) = \sum_{k=1}^{N} r_k(t)\frac{V_f^{t^{k-1}g}(t,\xi)}{V_f^g(t,\xi)} = \frac{1}{i2\pi}[\log(A)]'(t) + \phi'(t) + \sum_{k=2}^{N} r_k(t)\frac{V_f^{t^{k-1}g}(t,\xi)}{V_f^g(t,\xi)}, \tag{13}$$

where $r_k(t) = \frac{1}{(k-1)!}\left(\frac{1}{i2\pi}[\log(A)]^{(k)}(t) + \phi^{(k)}(t)\right)$. It is clear that to get an exact IF estimate for the studied signal, one needs to subtract $\Re\left\{\sum_{k=2}^{N} r_k(t)\frac{V_f^{t^{k-1}g}(t,\xi)}{V_f^g(t,\xi)}\right\}$ to $\Re\{\tilde{\omega}_f(t,\xi)\}$, which requires the calculation of $r_k(t)$ for $k = 2,\ldots,N$. For that purpose, one derives a frequency modulation operator $\tilde{q}_f^{[k,N]}(t,\xi)$, equal to $r_k(t)$ for the type of modes just introduced, and the definition of the $\mathrm{N^{th}}$-order IF estimate then follows [17]:

$$\tilde{\omega}_f^{[N]}(t,\xi) = \begin{cases} \tilde{\omega}_f(t,\xi) + \sum_{k=2}^{N} \tilde{q}_f^{[k,N]}(\xi,t)\left(-x_{k,1}(t,\xi)\right), \\ \text{if } V_f^g(t,\xi) \neq 0, \text{ and } \partial_\xi x_{j,j-1}(t,\xi) \neq 0, \\ \qquad\qquad 2 \leq j \leq N \\ \tilde{\omega}_f(t,\xi) \qquad \text{otherwise.} \end{cases}$$

with $x_{k,1}(t,\xi) = \frac{V_f^{t^{k-1}g}(t,\xi)}{V_f^g(t,\xi)}$. $\hat{\omega}_f^{[N]}(t,\xi) = \Re\{\tilde{\omega}_f^{[N]}(t,\xi)\}$ is then the desired IF estimate which is, by construction, exact for f satisfying (12). As for FSST2, the N^{th}-order FSST (FSSTN) is defined by replacing $\hat{\omega}_f(t,\xi)$ by $\hat{\omega}_f^{[N]}(t,\xi)$ in (7) to obtain $T_{N,f}^{\gamma}(t,\omega)$ and the modes of the MCS can be reconstructed by replacing $T_f^{\gamma}(t,\omega)$ by $T_{N,f}^{\gamma}(t,\omega)$ in (8).

III. Demodulation Algorithm Based On Higher Order FSST for Mode Reconstruction

In this section, we recall the concept of the demodulation algorithm based on FSST (or FSST2) which was introduced in [16]. Then, we propose a variant of this algorithm that we coin DFSSTN in the sequel and show how the use of FSSTN results in better IF estimation and improved mode reconstruction by means of demodulation. The demodulation algorithm is based on a ridge extraction technique from the reassigned transform which we first recall.

A. Ridge Estimation

Any mode reconstruction technique based on the synchrosqueezing transform requires an estimate of the ridges $(t, \phi_k'(t))$, for which, assuming knowledge of the number K of modes, we use the same algorithm as in [8] or [6], and originally proposed in [19]. This computes a local minimum of the functional

$$E_f(\psi_1,\cdots,\psi_K) = \sum_{k=1}^{K} -\int_{\mathbb{R}} |TF_f(t,\psi_k(t))|^2 + \lambda\psi_k'(t)^2 + \beta\psi_k''(t)^2 dt,$$

where TF_f is one of the TF representations introduced above, i.e. FSST, FSST2, or FSSTN. In [16], it was shown that to use regularization parameters λ and β did not bring any improvement in terms of ridge detection (especially when synchrosqueezed transforms are considered), so we set them to zero.

B. Mode Reconstruction with Demodulation Based on Higher Order Synchrosqueezing (DFSSTN)

The previous section has provided us with a means to extract the ridges from the reassigned transforms, and these correspond to piecewise constant approximations of the IFs of the modes which are subsequently used in the mode reconstruction by putting $\varphi_k(t) = \psi_k(t)$ for $k = 1,\cdots,K$. In [16], these IFs estimates were used in a demodulation algorithm but the obtained results, though encouraging, were strongly dependent on the frequency resolution when computing STFT. Indeed, assume f is with finite length, typically defined on the interval $[0,T]$, discretized into $f(\frac{nT}{R})_{n=0,\cdots,R-1}$, and g supported on $[-\frac{LT}{R}, \frac{LT}{R}]$ with $L < R/2$, the STFT of f is then computed as follows:

$$V_f^g(t,\xi) = \int_{-\frac{LT}{R}}^{\frac{LT}{R}} f(t+\tau)g(\tau)e^{-2i\pi\tau\xi}d\tau \approx \frac{T}{R}\sum_{n=-L}^{L} f\left(t+\frac{nT}{R}\right)g\left(\frac{nT}{R}\right)e^{-i2\pi\frac{nT}{R}\xi}, \tag{14}$$

from which we infer that, for $0 \leq p \leq R-1$:

$$V_f^g\left(\frac{qT}{R}, \frac{pR}{MT}\right) \approx \frac{T}{R}\sum_{n=-L}^{L} f\left(\frac{(q+n)T}{R}\right)g\left(\frac{nT}{R}\right)e^{-i2\pi\frac{np}{M}},$$

for some $M \geq 2L+1$. The last sum is computed by means of a discrete Fourier transform, and the frequency resolution equals $\frac{R}{MT}$. This has the consequence that STFT is all the more compact that the frequency resolution is low, and that the IFs estimation based on crude ridges extraction is very inaccurate in that case.

We now propose to use, for the purpose of mode reconstruction using a demodulation algorithm, much more relevant IFs estimates than those based on crude ridges extraction. Indeed, while performing FSST, FSST2, or FSSTN, one computes $\hat{\omega}_f(t,\xi)$, $\hat{\omega}_f^{[2]}(t,\xi)$, and $\hat{\omega}_f^{[N]}(t,\xi)$, respectively. These, evaluated on the ridge associated with the kth mode, i.e. $\hat{\omega}_f(t,\varphi_k(t))$, $\hat{\omega}_f^{[2]}(t,\varphi_k(t))$, and $\hat{\omega}_f^{[N]}(t,\varphi_k(t))$, lead to much smoother IF estimates than those proposed in [16]. Based on the IFs estimates we use the demodulation procedure proposed in [16] (see Algorithm 1).

Algorithm 1 Demodulation based on FSSTN (DFSSTN)

Estimate the ridges $(\psi_1,\cdots,\psi_K)$ from FSSTN.

for $k=1$ to K **do**

1. Compute $\tilde{\varphi}_k(t)=\hat{\omega}_f^{[N]}(t,\psi_k(t))$.
2. Compute $f_{D,k}(t)=f(t)e^{-i2\pi(\int_0^t\tilde{\varphi}_k(x)dx-\psi_0 t)}$.
3. From $T^{\gamma}_{f_{D,k}}$, extract the ridge $\psi_{D,k}$ corresponding to mode k of $f_{D,k}$, by considering single ridge detection in $[\psi_0-\Delta,\psi_0+\Delta]$.
4. Reconstruct the kth mode of $f_{D,k}$ and then multiply it by the inverse of demodulation operator to recover f_k: $f_k(t)\approx\left(\int_{|\omega-\psi_{D,k}(t)|<d}T^{\gamma}_{f_{D,k}}(t,\omega)d\omega\right)e^{i2\pi(\int_0^t\tilde{\varphi}_k(x)dx-\psi_0 t)}$.

IV. Results and Discussion

This section provides some numerical experiments on an MCS, in both noise-free and noisy cases, illustrating the benefits of using Algorithm 1, with N = 3 or 4, rather than other existing techniques including FSST2, FSST3, FSST4 [17] and DFSST2 [16]. The MATLAB scripts generating all the figures of this paper can be downloaded from *github.com/phamduonghung/EUSIPCO2019*.

Let us first consider a synthetic MCS composed of two AM-FM modes defined as: $f(t)=f_1(t)+f_2(t)$ with $f_1(t)=e^{2(1-t)^3}e^{i2\pi(50t+30t^3-20(1-t)^4)}$ and $f_2(t)=(1+7(1-t)^4)e^{i2\pi(340t-2e^{-2(t-0.2)}\sin(14\pi(t-0.2)))}$, for $t\in[0,1]$. Note that f_1 is a polynomial chirp fitting in the model defined by (11) and f_2 is a damped-sine function containing very strong nonlinear sinusoidal frequency modulations. Such a signal is sampled at a rate $R=1024$ Hz on $[0,1]$. We use the L^1-normalized Gaussian window $g(t)=\sigma^{-1}e^{-\pi\frac{t^2}{\sigma^2}}$ to compute the STFT of f, where σ is the optimal value determined minimizing Rényi entropy [20].

In Figure 1, we depict the modulus of STFT and close-ups of reassigned representations given by FSST2, FSST3, FSST4, respectively. It is clear that all the studied techniques lead to relatively sharp TFRs for this mode (f_1 behaves locally as a Gaussian modulated linear chirp). In contrast, for f_2, the higher the order of FSST the sharper the TFR; especially when the IF of the mode has a non negligible *curvature* $\phi''(t)$. It was shown in [17] that the better TF concentration when using FSSTN also meant better mode reconstruction performance. However, the latter can be further improved by using DFSSTN as shown hereafter, in noise-free and noisy situations.

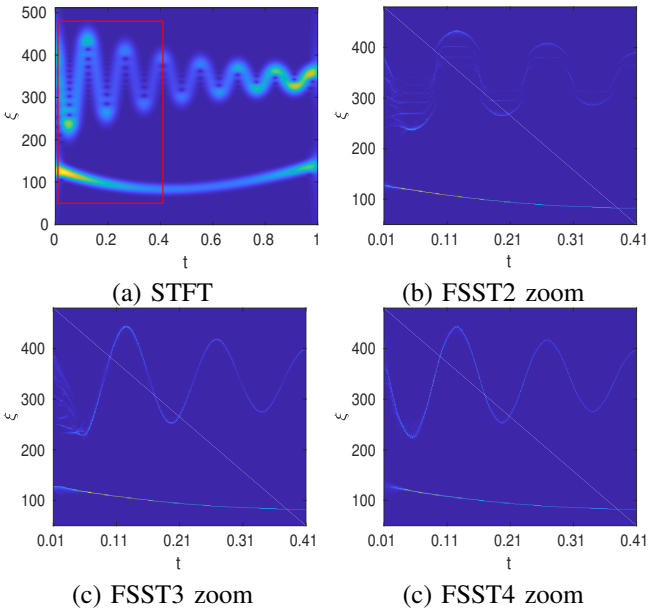

Fig. 1. (a): modulus of the STFT of f with a small patch (delimited by a red rectangle); (b): zoom in FSST2 computed from the patched STFT shown in (a); from (c) to (d), same as (b) but for FSST3 and FSST4 respectively.

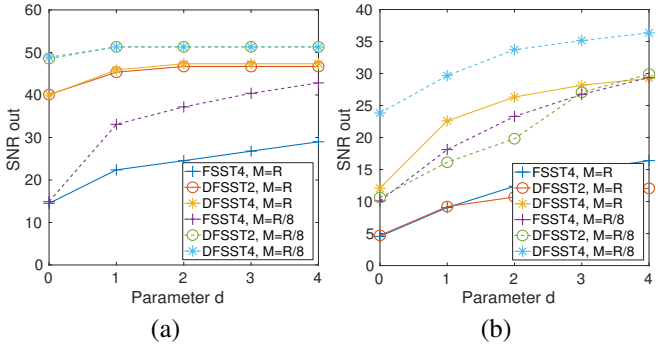

Fig. 2. Noise-free case: (a) reconstruction accuracy measured by ouput SNR with respect to d for mode f_1 using FSST4, DFSST2 and DFSST4 (with $M=R$ and $M=R/8$); (b): same as (a) but for mode f_2.

A. Noise-Free Case

We display, in Figures 2 (a) and (b), the quality of retrieval processes associated with f_1 and f_2, respectively, with respect to parameter d defined in (8), using FSST4, DFSST2 and DFSST4 computed either with $M=R$ and $M=R/8=128$. It is worth noting that, in our simulations, the optimal σ as determined above leads to a filter length $2L+1=123$, and $M=R/8=128$ is close to the smallest value one can choose. Besides, the performance of mode reconstruction are evaluated by $\text{SNR}_{\text{out}}=20\log_{10}\left(\|f_k\|_2/\|f_{k,r}-f_k\|_2\right)$, where $f_{k,r}$ is the kth reconstructed mode and $\|.\|_2$ is the l_2 norm. We first remark from Figure 2 that a bigger d results in better reconstruction qualities, which is consistent with earlier research [16], [18]. Moreover, it can be seen that the tested techniques computed with $M=R/8$ (low frequency resolution) perform much better than those calculated with higher frequency resolution $M=R$: a compact representation

should clearly be favored. Finally, yet most importantly, for each M used, while DFSST4 produces quite similar results to DFSST2, these are much better than those obtained with FSST4 for f_1. For mode f_2, DFSST4, taking into account the curvature in the demodulation operator, outperforms all the other studied techniques.

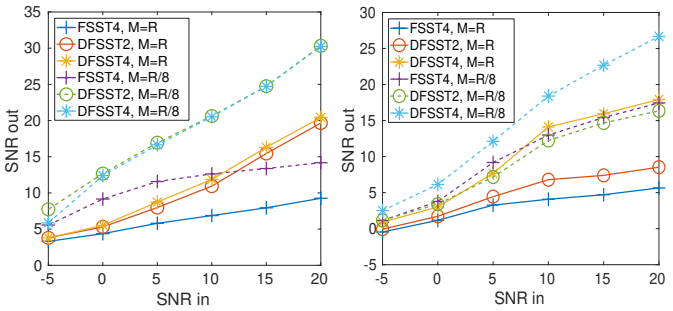

(a): mode f_1 (b): mode f_2

Fig. 3. In a noise-free case: (a) reconstruction accuracy measured using output SNR with respect to different input SNR for f_1 using FSST4, DFSST2 and DFSST4 computed with both $M = R$ and $M = R/8$ and choosing $d = 1$; (b): same as (a) but for f_2.

B. Noisy Case

To further challenge the different tested techniques in the presence of noise, we consider a noisy signal defined $f_\zeta(t) = f(t) + \zeta(t)$, where $\zeta(t)$ is a complex white Gaussian process with variance $\mathrm{Var}\left(\Re\left\{\zeta(t)\right\}\right) = \mathrm{Var}\left(\Im\left\{\zeta(t)\right\}\right) = \sigma_\zeta^2$, where $\Re\{Z\}$ and $\Im\{Z\}$ stand for the real and imaginary parts of complex number Z. Furthermore, the noise level is measured by: $\mathrm{SNR}_{\mathrm{in}}[\mathrm{dB}] = 20\log_{10}\left(\|f\|_2 / \|f_\zeta - f\|_2\right)$. Then, we again investigate the reconstruction qualities for modes f_1 and f_2, for FSST4, DFSST2 and DFSST4, when $M = R$ or $M = R/8 = 128$ and with $d = 1$. Note that these qualities are the means of the reconstruction accuracies obtained by repeating each simulation 100 times. As in the previous case, DFSST4 still exhibits the best mode reconstruction performance, as reported in Figure 3 (a) and (b). To conclude, our simulations plead in favor of using FSSTN, with a low frequency resolution, followed by a demodulation procedure (DFSSTN) to reconstruct the modes of an MCS rather than FSSTN alone or DFSST2.

V. Conclusion

In this paper, we have introduced a new technique for the retrieval of the modes of multicomponent signals from their time-frequency representation, based on high-order synchrosqueezing transforms (FSSTN) together with a demodulation procedure. Numerical experiments demonstrated the improvement brought by the proposed technique over state-of-the-art methods for both noise-free and noisy signals. Future work should now be devoted to a more theoretical analysis of the proposed techniques in more general noisy situations, including both Gaussian and non-Gaussian noises, as was done in [21], [22] for synchrosqueezing transforms.

References

[1] M. Costa, A. A. Priplata, L. A. Lipsitz, Z. Wu, N. E. Huang, A. L. Goldberger, and C.-K. Peng, "Noise and poise: Enhancement of postural complexity in the elderly with a stochastic-resonance-based therapy," *Europhysics Letters (EPL)*, vol. 77, no. 6, p. 68008, Mar 2007.

[2] D. A. Cummings, R. A. Irizarry, N. E. Huang, T. P. Endy, A. Nisalak, K. Ungchusak, and D. S. Burke, "Travelling waves in the occurrence of dengue haemorrhagic fever in Thailand," *Nature*, vol. 427, no. 6972, pp. 344 –347, Jan 2004.

[3] C. L. Herry, M. Frasch, A. J. Seely, and H.-T. Wu, "Heart beat classification from single-lead ecg using the synchrosqueezing transform," *Physiological Measurement*, vol. 38, no. 2, pp. 171–187, 2017.

[4] P. Flandrin, *Time-frequency/time-scale analysis*. Academic Press, 1998, vol. 10.

[5] K. Kodera, R. Gendrin, and C. Villedary, "Analysis of time-varying signals with small bt values," *IEEE Transactions on Acoustics, Speech, and Signal Processing*, vol. 26, no. 1, pp. 64–76, Feb 1978.

[6] F. Auger and P. Flandrin, "Improving the readability of time-frequency and time-scale representations by the reassignment method," *IEEE Transactions on Signal Processing*, vol. 43, no. 5, pp. 1068–1089, 1995.

[7] I. Daubechies and S. Maes, "A nonlinear squeezing of the continuous wavelet transform based on auditory nerve models," *Wavelets in medicine and biology*, pp. 527–546, 1996.

[8] I. Daubechies, J. Lu, and H.-T. Wu, "Synchrosqueezed wavelet transforms: an empirical mode decomposition-like tool," *Applied and Computational Harmonic Analysis*, vol. 30, no. 2, pp. 243–261, 2011.

[9] G. Thakur and H.-T. Wu, "Synchrosqueezing-based recovery of instantaneous frequency from nonuniform samples." *SIAM J. Math. Analysis*, vol. 43, no. 5, pp. 2078–2095, 2011.

[10] M. Skolnik, *Radar Handbook*, Technology and Engineering, Eds. McGraw-Hill Education, 2008.

[11] J. W. Pitton, L. E. Atlas, and P. J. Loughlin, "Applications of positive time-frequency distributions to speech processing," *IEEE Transactions on Speech and Audio Processing*, vol. 2, no. 4, pp. 554–566, 1994.

[12] E. J. Candes, P. R. Charlton, and H. Helgason, "Detecting highly oscillatory signals by chirplet path pursuit," *Applied and Computational Harmonic Analysis*, vol. 24, no. 1, pp. 14–40, 2008.

[13] B. P. Abbott, R. Abbott, T. Abbott, M. Abernathy, F. Acernese, K. Ackley, C. Adams, T. Adams, P. Addesso, R. Adhikari *et al.*, "Observation of gravitational waves from a binary black hole merger," *Physical review letters*, vol. 116, no. 6, p. 061102, 2016.

[14] T. Oberlin, S. Meignen, and V. Perrier, "The Fourier-based synchrosqueezing transform," in *2014 IEEE International Conference on Acoustics, Speech and Signal Processing (ICASSP)*, May 2014, pp. 315–319.

[15] R. Behera, S. Meignen, and T. Oberlin, "Theoretical analysis of the second-order synchrosqueezing transform," *Applied and Computational Harmonic Analysis*, vol. 45, no. 2, pp. 379–404, Sep 2018.

[16] S. Meignen, D.-H. Pham, and S. McLaughlin, "On demodulation, ridge detection and synchrosqueezing for multicomponent signals," *IEEE Transactions on Signal Processing*, vol. 65, no. 8, pp. 2093–2103, 2017.

[17] D.-H. Pham and S. Meignen, "High-order synchrosqueezing transform for multicomponent signals analysis - with an application to gravitational-wave signal," *IEEE Transactions on Signal Processing*, vol. 65, no. 12, pp. 3168–3178, June 2017.

[18] T. Oberlin, S. Meignen, and V. Perrier, "Second-order synchrosqueezing transform or invertible reassignment? Towards ideal time-frequency representations," *IEEE Transactions on Signal Processing*, vol. 63, no. 5, pp. 1335–1344, March 2015.

[19] R. Carmona, W. Hwang, and B. Torresani, "Characterization of signals by the ridges of their wavelet transforms," *IEEE Transactions on Signal Processing*, vol. 45, no. 10, pp. 2586–2590, Oct 1997.

[20] L. Stanković, "A measure of some time–frequency distributions concentration," *Signal Processing*, vol. 81, no. 3, pp. 621–631, 2001.

[21] G. Thakur, E. Brevdo, N. S. FučKar, and H.-T. Wu, "The synchrosqueezing algorithm for time-varying spectral analysis: Robustness properties and new paleoclimate applications," *Signal Processing*, vol. 93, no. 5, pp. 1079–1094, May 2013.

[22] H. Yang, "Statistical analysis of synchrosqueezed transforms," *Applied and Computational Harmonic Analysis*, Jan. 2017.